



Published in final edited form as:

*Biomaterials*. 2019 April ; 200: 15–24. doi:10.1016/j.biomaterials.2019.02.004.

## Varying PEG density to control stress relaxation in alginate-PEG hydrogels for 3D cell culture studies

Sungmin Nam<sup>1</sup>, Ryan Stowers<sup>1</sup>, Junzhe Lou<sup>2,3</sup>, Yan Xia<sup>2</sup>, and Ovijit Chaudhuri<sup>1,\*</sup>

<sup>1</sup>Department of Mechanical Engineering, Stanford University, CA, USA.

<sup>2</sup>Department of Chemistry, Stanford University, CA, USA.

<sup>3</sup>Department of Materials Science and Engineering, Stanford University, CA, USA.

### Abstract

Hydrogels are commonly used as artificial extracellular matrices for 3D cell culture and for tissue engineering. Viscoelastic hydrogels with tunable stress relaxation have recently been developed, and stress relaxation in the hydrogels has been found to play a key role in regulating cell behaviors such as differentiation, spreading, and proliferation. Here we report a simple but precise materials approach to tuning stress relaxation of alginate hydrogels with polyethylene glycol (PEG) covalently grafted onto the alginate. Hydrogel relaxation was modulated independent of the initial elastic modulus by varying molecular weight and concentration of PEG along with calcium crosslinking of the alginate. Increased concentration and molecular weight of the PEG resulted in faster stress relaxation, a higher loss modulus, and increased creep. Interestingly, we found that stress relaxation of the hydrogels is determined by the total mass amount of PEG in the hydrogel, and not the molecular weight or concentration of PEG chains alone. We then evaluated the utility of these hydrogels for 3D cell culture. Faster relaxation in RGD-coupled alginate-PEG hydrogels led to increased spreading and proliferation of fibroblasts, and enhanced osteogenic differentiation of mesenchymal stem cells (MSCs). Thus, this work establishes a new materials approach to tuning stress relaxation in alginate hydrogels for 3D cell culture.

### Keywords

Hydrogels; 3D cell culture; Viscoelasticity; Stress relaxation; PEG

\*Correspondence to: [chaudhuri@stanford.edu](mailto:chaudhuri@stanford.edu).

#### Author Contributions

S.N., R.S., J.L., Y.X., and O.C. designed the experiments. S.N., R.S., J.L., and O.C. analyzed the data. S.N., R.S., and J.L. conducted the experiments. S.N. and O.C. wrote the manuscript.

**Publisher's Disclaimer:** This is a PDF file of an unedited manuscript that has been accepted for publication. As a service to our customers we are providing this early version of the manuscript. The manuscript will undergo copyediting, typesetting, and review of the resulting proof before it is published in its final citable form. Please note that during the production process errors may be discovered which could affect the content, and all legal disclaimers that apply to the journal pertain.

#### Data Availability

The raw data required to reproduce these findings are available upon request. The processed data required to reproduce these findings are available upon request.

## Introduction

Hydrogels are commonly used as artificial ECMs to mimic physiological environments and understand cell-matrix interactions, and as cell-laden biomaterial implants to improve tissue regeneration [1–5]. It has been established that cells sense and respond to the mechanical properties of hydrogels. Studies investigating the impact of mechanical properties of hydrogels on cells have found that the elastic modulus of hydrogels plays a key role in regulating cell spreading, promoting proliferation, and determining stem cell fate [6–10]. Natural ECM is also viscoelastic and exhibits stress relaxation, with the resistance to a deformation relaxing over time [11,12]. Recently, an emerging body of work has demonstrated that the stress relaxation or creep properties of viscoelastic hydrogels also impact cell behaviors such as migration, spreading, proliferation, and differentiation [11,13–20]. Thus, there is a need for hydrogels in which the initial elastic modulus and stress relaxation properties can be independently modulated.

While a number of approaches to control viscoelasticity of various hydrogel materials have been reported, these often require complex chemical processing. Stress relaxation in hydrogels can arise from weak crosslinking of the polymer structure in the hydrogel [12,21,22]. Thus, hydrogels exhibiting stress relaxation can be formed through use of ionic crosslinking in alginate gels [11], hydrogen bonding in supramolecular polymers [23], guest-host bonding in hyaluronic acid gels [24], and reversible covalent bonding in PEG gels [14,16], hyaluronic acid-collagen gels [15], and furan and maleimide polymer-based gels [25]. Stress relaxation in such hydrogels can be tuned by varying the functionality and structure of crosslinks [14,15,21,26], polymer architecture or density along with crosslink density [19], and the addition of a catalyst to modulate the exchange rate of crosslinks [27]. For example, in ionically crosslinked alginate hydrogels, decreasing the molecular weight while increasing the density of ionic crosslinks altered network connectivity and enhance chain mobility, thereby allowing faster hydrogel relaxation [11]. Alternatively, covalent grafting short PEG chains to the alginate was also demonstrated to promote faster stress relaxation, with the PEG chains serving as a steric hindrance to crosslinking of the alginate chains [11]. While many approaches have been established, some of the crosslinking chemistries involve complex processing, and the range of molecular weights available commercially for alginate are limited. Therefore, a simple but precise method to control hydrogel stress relaxation over a wide window is desired.

Here, we report a straightforward but efficient strategy to control viscoelasticity of alginate hydrogels, independently of an initial elastic modulus, through modification of PEG coupling to the alginate. We rigorously study the impact of PEG grafting on the stress relaxation of alginate hydrogels, by varying the concentration and molecular weight of PEG grafted onto the alginate. We find that hydrogel stress relaxation is determined by the total mass amount of PEG in the gels, and not the concentration or molecular weight of PEG alone. Next, we used the alginate-PEG gels as a three-dimensional (3D) cell culture platform. Faster stress relaxation in the alginate-PEG hydrogels promotes cells spreading, proliferation, and osteogenesis, demonstrating the utility of this material system for 3D cell culture.

## Materials and methods

### 1) Alginate preparation

Sodium alginate rich in guluronic acid blocks and with a high molecular weight (280 kDa, LF20/40) was purchased from FMC Biopolymer, and was prepared as has been described previously [11]. Alginate was dialyzed against deionized water for 2–3 days, filtered with activated charcoal, lyophilized, and then reconstituted at 3 wt% in phosphate-buffered saline (PBS) or serum-free Dulbecco's modified Eagle's medium (DMEM).

### 2) PEG/RGD modification of alginate

Alginate-PEG was prepared by grafting PEG-amine to alginate using carbodiimide chemistry [11] at the concentration, as described in Supplementary table 2. PEG-amine was mixed with 20 ml of 10 mg ml<sup>-1</sup> alginate in 0.1 M MES (2-(N-morpholino) ethane sulfonic acid, Sigma-Aldrich) buffer at pH 6.5. Then the appropriate amount of EDC (N-(3-dimethylaminopropyl)-N'-ethyl carbodiimide hydrochloride, Sigma-Aldrich) and Sulfo-NHS (N-hydroxysulphosuccinimide, Thermo Fisher Scientific) were added into the solution (Supplementary table 2). A 280 kDa alginate was used to react with PEGs at different lengths and the amount of added PEG was determined based on the targeted degree of substitution and estimating 60 % of added PEG to be grafted onto alginate, following our previous observation in similar systems [11]. The reaction was carried out for 20 h under constant stirring. The product was dialyzed against sodium chloride solution with gradually decreasing concentration for three days and lyophilized. The structure of the PEG–alginate was confirmed with nuclear magnetic resonance (NMR) spectroscopy. Alginate-RGD was prepared by coupling the oligopeptide GGGGRGDSP (Peptides International) to alginate using carbodiimide chemistry at a final concentration of 1500 μM with a similar procedure to the PEG coupling [11]. After modifying alginate with RGD, PEG was further coupled to the alginate-RGD with the procedure, as described above.

### 3) NMR analysis

Quantitative analysis of PEG modification was performed on nuclear magnetic resonance (NMR, D<sub>2</sub>O, 500 MHz) spectroscopy by using internal standard method [28]. Potassium hydrogen phthalate (KHP) was chosen as the internal standard ( $\delta$  at 7.50 ppm) and prepared in the same solution with the analytes at a constant concentration of 0.4 wt%. First, a standard curve was plotted using the integration ratio of 1H NMR peak area between 0.4 wt % KHP ( $\delta$  at 7.50 ppm) and ethylene units on pristine PEG (varied from 0.05 wt% to 0.4 wt %,  $\delta$  at 3.56 ppm). All analyzed samples prepared for the standard curve contained 0.8 wt% of pristine alginate. PEG-grafted alginate samples were then dissolved at 0.8 wt% in D<sub>2</sub>O solvent containing 0.4 wt % of KHP. The concentrations of PEG in those samples were quantified by correlating the integration ratio of 1H NMR peak area between KHP and PEG grafted on alginate to the standard curve. The molar ratio between PEG and alginate in these samples were calculated according to their mass fraction and molecular weight, indicating the efficiency of PEG modification.

#### 4) Mechanical characterization

Rheological measurements were performed with an AR-G2 stress-controlled rheometer (TA Instruments), equipped with 25-mm top and bottom plate geometry. Alginate gels were deposited onto the bottom plate of the rheometer immediately after mixing with the crosslinker. The top plate was rapidly brought down so that the gels formed a uniform disk between the rheometer plates. The exposed gel surface was enclosed by mineral oil (Sigma Aldrich) to prevent dehydration of the gels. The storage modulus of gels was monitored at a strain of 0.01 and frequency of  $1 \text{ rad s}^{-1}$ . The elastic modulus reported in this study was calculated by converting shear modulus,  $E = 2G(1 + \nu)$ , where  $E$ ,  $G$ , and  $\nu$  are elastic modulus, shear modulus, and Poisson ratio respectively. The Poisson ratio was assumed to be 0.45 as in previous studies [29]. Mechanical tests, including stress relaxation, oscillatory, and creep tests, were performed once the storage modulus reached an equilibrium value. For stress relaxation tests, a strain of 0.1, 0.2, 0.25 was applied to the samples with a rise time of 0.1 s. While the strain was held constant, stress was recorded over time. The stress relaxation time was quantified as the time at which the initial stress of the gels was relaxed to half of its initial value. For oscillatory tests, a strain of 0.01 was applied while varying frequency from  $10^{-4}$  to 1 Hz. For creep tests, a constant stress of 100 – 150 Pa was applied to the samples.

Unconfined compression stress relaxation tests were performed using a mechanical tester (Instron, 5848 MicroTester). Alginate gel disks (6 mm in diameter, 2 mm thick) were formed and equilibrated in DMEM for 24 hours. The alginate gel disks were placed on the machine and compressed to a strain of 20% at a deformation rate of  $1 \text{ mm mm}^{-1}$ .

#### 5) Cell culture and encapsulation

3T3 fibroblasts transfected with RFP-actin were cultured in standard Dulbecco's Modified Eagles Medium (DMEM, Invitrogen) with 10% Fetal Bovine Serum (Invitrogen) and 1% penicillin/streptomycin (Invitrogen). D1 mouse MSCs (ATCC) were expanded in DMEM containing 10% Fetal Bovine Serum and 1% Pen/Strep. The medium was changed every 2–3 days and the cells were passaged at 70 % confluency.

For cell encapsulation in hydrogels, cells were first trypsinized, washed in serum-free DMEM, and re-suspended as a single cell suspension in serum-free DMEM. The concentration of cells was measured using a Vi-Cell (Beckman Coulter). For cell spreading and proliferation experiments, 3T3 were encapsulated in gels at the final concentration of 2–3 million cells per mL. For differentiation experiments, D1 cells were encapsulated in gels at the final concentration of 9–10 million cells per mL. Cells were then mixed with alginate reconstituted in serum-free DMEM in one Luer lock syringe (Cole-Parmer). The cell-alginate solution in the syringe was homogeneously mixed with DMEM containing the appropriate concentration of calcium sulfate in another syringe, connected by a female-female coupler (Value-plastics). The mixed solution was deposited between two glass plates spaced 2 mm apart, allowed to gel for 45 minutes, and then punched out with a 6 mm diameter biopsy punch, resulting in the total volume of gels to be  $\sim 57 \text{ mm}^3$ . The gels were transferred to well plates and immersed in cell culture media.

## 6) Characterization of gel degradation/swelling ratio

To assess degradation and swelling of hydrogels, gels were formed with a diameter of 6 mm and a height of 2 mm, as described above. Gels were then incubated in culture media for one day or a week. For characterization of gel degradation, gels incubated for one day and a week were frozen and lyophilized. The dry mass of the hydrogels was then measured. Degradation was assessed by comparing the dry mass of the hydrogels after one week to the value after one day. For characterization of gel swelling, gels incubated for a week were removed from the medium, and the wet and dry mass of gels was measured. Swelling was quantified as the ratio of the wet mass of the gels to the dry mass.

## 7) Immunohistochemical staining

For immunohistochemical staining, cells were encapsulated in hydrogels and cultured for 7 days, and the gels containing cells were fixed with 4% paraformaldehyde in serum-free DMEM at 37 °C for 30–45 min. The gels were then washed three times in PBS containing calcium (cPBS, GE), and incubated in 30% sucrose (Fischer Scientific) at 4°C overnight. The gels were placed in a mix of 50% of a 30% sucrose in cPBS solution, and 50% OCT (Tissue-Tek) for 4 hours. The gels were then embedded in OCT, frozen, and sectioned with a thickness of 30–80 µm using a cryostat (Leica CM1950). The sectioned samples were stained using standard immunohistochemistry protocols. The following antibodies/reagents were used for immunohistochemistry: paxillin antibody (Abcam, ab32084), β1 integrin antibody (Abcam, ab24693), and Prolong Gold antifade reagent with DAPI (Invitrogen). The Click-IT EdU cell proliferation assay (Invitrogen) was used to assess the cell-cycle progression of cells.

## 8) Immunoblot

For immunoblot analysis, cells were encapsulated and cultured for one week and then harvested from gels. Cell-gel constructs were incubated in 50 mM EDTA (Sigma) to chelate calcium for 5 minutes with vigorous pipetting to break up the gels and then centrifuged for 10 minutes, and supernatant was removed. Cell were then lysed in Pierce RIPA buffer supplemented with Protease Inhibitor Cocktail Tablets (Roche) and PhosSTOP Phosphatase Inhibitor 858 Cocktail Tablets (Roche). Pierce BCA Protein Assay Kit (Thermo Fisher Scientific) was used to quantify the concentration of harvested protein from the cell lysates. The harvested proteins were mixed with Laemmli sample buffer (Bio-Rad) and boiled for 5 minutes and loaded in a polyacrylamide (PA) gradient gel (Bio-Rad). The proteins in the PA gels were transferred to nitrocellulose at 100V for 1 hour, incubated in primary antibodies overnight, and then incubated with IRDye 680-or 800-conjugated secondary antibodies for 1 hour. Li-COR Odyssey imaging system (Li-COR Biotechnology) was used to visualize the proteins in the nitrocellulose. Antibodies used for immunoblot were listed: p-FAK (Cell Signaling Technology), FAK (Invitrogen), p-paxillin (Cell Signaling Technology) and paxillin (Cell Signaling Technology).

## 9) Counting cell numbers in gels

To measure the number of cells in cell-gel constructs, cells were encapsulated and cultured for one week and then harvested by chelating calcium in gels. Gels containing cells were

incubated in cold-PBS containing 50 mM EDTA (Sigma) for 5 minutes to break up the gels and then centrifuged for 10 minutes, and supernatant was removed. The number of the harvested cells were then measured using a Vi-Cell instrument (Beckman Coulter).

#### 10) Gene expression analysis

For gene expression analysis, cells were encapsulated and cultured for one week, and then RNA in cells was harvested. Cell-gel constructs were ground and treated with cold PBS containing 50 mM EDTA with pipetting to break up the gels. A commercially available RNA extraction kit (Epoch) with TRIZOL (Invitrogen) was used to extract RNA. The harvested RNA was then transcribed to cDNA using a High-Capacity cDNA Reverse Transcription Kit (Thermofisher). The expression of osteogenic genes was measured using real-time polymerase chain reaction (PCR) with Fast SYBR green master mix (Applied Biosystems). Gene expression was reported as normalized to GAPDH. Primers used were listed in Supplementary Table 3.

#### 11) Differentiation assay

For differentiation experiments, D1 cells were encapsulated in gels, cultured for 7 days, and then fixed. The culture medium was supplemented with 50  $\mu\text{g ml}^{-1}$  L-ascorbic acid (Sigma), 10 mM  $\beta$ -glycerophosphate (Sigma) and 0.1  $\mu\text{M}$  dexamethasone (Sigma). The medium was changed every 2–3 days.

To assess osteogenic differentiation, alkaline phosphatase (ALP) was probed using the Fast Blue assay. First, hydrogels containing D1 cells were frozen and sectioned as described above. The sectioned gels were then equilibrated in alkaline buffer (100 mM Tris-HCl, 100 mM NaCl, 0.1% Tween-20, 50 mM  $\text{MgCl}_2$ , pH 8.2) for 15 min and stained in 500  $\mu\text{g ml}^{-1}$  naphthol AS-MX phosphate (Sigma) and 500  $\mu\text{g ml}^{-1}$  Fast Blue BB Salt Hemi ( $\text{ZnCl}_2$ ) salt (Sigma) in alkaline buffer for 60 min. The sections were then washed in alkaline buffer and equilibrated in PBS.

#### 12) Cell-cycle progression assay

For the cell-cycle progression assay, cells were first encapsulated in hydrogels and cultured for one day, and then EdU (Thermo Fisher Scientific) was added to the culture medium at a final concentration of 10  $\mu\text{M}$ . After 2 days of culture with EdU, cells were fixed and EdU was stained according to the manufacturer's instructions.

#### 13) Image analysis

All images were taken using a confocal microscope (Leica, SP8) with a 25 $\times$ /0.95 NA water immersion objective, except for color micrographs of Fast blue staining. Color micrographs of Fast Blue staining was obtained using Zeiss Axiovert 200M microscope and a Zeiss Axiocam 105 color camera.

Cell morphology parameters including roundness, solidity, and aspect ratio of single cells were quantified using Image J. In ImageJ, roundness is calculated as  $\frac{4A}{\pi L^2}$ , where A and L represent the area and the major length of cells, solidity as the area of cells divided by the



area of the smallest convex enclosure that contains the cells, and aspect ratio as the major length of cells divided by their minor length. The percentage of cells with colocalization of  $\beta$ 1-integrin and paxillin was determined by counting the number of cells with overlapping  $\beta$ 1-integrin and paxillin at protrusions.

#### 14) Statistical analysis

For statistical analysis, Student t-tests were used to compare two groups. One-way analysis of variance with Tukey's multiple comparison was used to compare more than two groups using GraphPad.

## Results

We first formed alginate-PEG hydrogels with different concentrations and molecular weights of PEG covalently coupled to the alginate (Fig. 1). Alginate hydrogels are commonly used for cell culture and tissue engineering due to its low cost and wide availability [30]. Monofunctional amine-terminated PEGs of short (2 kDa), medium (5 kDa), or long (20 kDa) length were grafted to the alginate using carbodiimide crosslinking chemistry, which is commonly used for conjugation of primary amine to carboxylic acid of alginate (Fig. 1) [30]. The number of PEG chains per alginate chain is defined as degree of substitution (DS), and we varied the DS for PEGs with the three different lengths to obtain two total masses of grafted PEG per alginate chain at 80 kDa (low density) or 160 kDa (high density). The number of PEG grafted per alginate chain was confirmed by nuclear magnetic resonance (NMR) spectroscopy (Supplementary Fig. 1; Supplementary Table 1). For this study, alginate polymer concentration in the alginate-PEG hydrogels was held constant at 20 mg/ml in the final gel in order to examine the impact of PEG-grafting alone.

We then investigated the impact of PEG number and length on the stress relaxation rate of the alginate-PEG hydrogels. Soft living tissues exhibit elastic moduli, related to stiffness, ranging from 100 Pa – 5 kPa [6]. Therefore, the initial modulus of gels was adjusted to ~ 3 kPa (Fig. 2A). First, the mechanics of gels containing alginate grafted with short PEG were examined with stress relaxation tests. In a stress relaxation test, a constant strain is applied to the hydrogels and the stress in response to strain is measured over time [11,12]. Gels from alginate with higher DS of PEG were found to exhibit faster stress relaxation (Fig. 2, B and C). Specifically, the time over which the initial stress was relaxed to half its value, defined as relaxation time, was modulated by the varying DS of PEG from a few hours to a few minutes (Fig. 2C). This range of timescales is comparable to the timescale of stress relaxation in physiological tissues, as reported previously [11]. Similarly, gels grafted with medium and long PEGs exhibited faster relaxation with increasing number of PEG (Fig. 2, D-I). In addition, stress relaxation tests at other strains and under compression was performed, and it was confirmed that the grafting PEG to alginate lead to faster stress relaxation across all the strains and also under compression (Supplementary Fig. 2). The dry mass of the gels was maintained over a few days, indicating that degradation of the gels is negligible over that timescale, and the swelling of the gels was not affected by the PEG grafting (Supplementary Fig. 3). These results show that increasing DS of PEG leads to faster relaxation in alginate-PEG gels.

We next asked what specific parameters control the rate of stress relaxation of the alginate-PEG gels. To examine how the rate of stress relaxation of the hydrogels depends on the concentration and length of PEG, we displayed relaxation time of all the hydrogels as a function of the DS or length of PEG (Fig. 3, A and B). Although increasing DS or length of PEG in the gels tended to enhance stress relaxation, neither the DS or length of PEG alone determined the relaxation time of all the hydrogels, given the scatter in the relaxation times as a function of PEG DS or length. Interestingly, the total amount of PEG, the product of the DS and length of PEG, was found to determine the relaxation time of the gels (Fig. 3C). Further, we displayed the loss tangent, a measure of viscosity that is defined as the ratio of loss modulus to storage modulus, as a function of the DS, length, or the total amount of PEG (Fig. 3, D-F). Consistent with the stress relaxation results, the loss tangent was found to be determined by the total amount of PEG. New formulations, using total amounts of PEG that lie between 0 and 160 kDa, would be expected to have stress relaxation times and loss tangents that fall along the equation derived from the experimental data (Fig. 3C and F). These results establish the total amount of PEG grafted onto alginate as the key parameter in modulating hydrogel stress relaxation and viscosity.

Next, we determined the creep properties and frequency-dependent rheology of the hydrogels. Creep and frequency dependent rheology tests are other standard methods used to characterize viscoelasticity in materials. Under a creep test, a material is initially strained in elastic response to a stress, and then the strain gradually increases over time due to the viscoelastic behavior of the material [31]. All the hydrogels initially showed a similar level of elastic strain, but the gels with higher PEG concentration exhibited a higher degree of viscoelastic creep over time (Fig. 4, A-C). Additionally, frequency-dependent rheology tests demonstrated that the loss modulus of hydrogels increased with higher PEG concentration (Fig. 4, D-F). Taken together, these results indicate that PEG-grafting leads to faster stress relaxation, greater creep, and a higher loss modulus in the alginate-PEG gels.

After establishing the viscoelastic properties of alginate-PEG hydrogels, we evaluated the utility of these gels as a 3D cell culture platform. As alginate and PEG do not carry intrinsic integrin-binding sites for mammalian cells, RGD was coupled to alginate-PEG to allow cell adhesion [11,32]. For cell culture studies, 5kDa PEG was chosen, since hydrogel relaxation is mainly determined by the total amount of PEG and PEG of 5kDa was the intermediate length among the various lengths of PEG. First, cell morphology was investigated. 3T3 fibroblasts were encapsulated within RGD-coupled alginate-PEG gels with an initial modulus of ~ 3 kPa and varying stress relaxation. In the gels with low concentration of PEG, corresponding to slow relaxation, cell spreading was inhibited and rounded morphologies were observed (Fig. 5A). In contrast, cells in the gels with higher PEG concentration, corresponding to fast relaxation, were found to spread more (Fig. 5A). This was confirmed by quantification of cell morphology (Fig. 5, B-D). The inclusion of cells did not alter stress relaxation of the gels (Supplementary Fig. 4). Next, proliferation was assessed. Cell-cycle progression of cells, measured by nuclear staining of EdU, was enhanced in the gels with faster relaxation, or a higher concentration of PEG, but reduced in the gels that exhibited slow stress relaxation (Fig. 5E and F). The number of cells in the gels were also measured after a week of culture. The number of cells in alginate-PEG gels is significantly higher than that in alginate gels (Supplementary Fig. 5). Together with the EdU findings, this indicates



that cells in alginate-PEG gels are more proliferative relative to cells in alginate gels. These results reveal that faster relaxation promotes cell spreading and proliferation in the alginate-PEG gels, consistent with previous 3D culture studies [11,14].

In addition to assessing spreading and proliferation of 3T3 cells, we looked at the formation of integrin-based adhesions. It is known that cells bind to ECM ligands through  $\beta$ 1-integrin and form focal adhesions through focal adhesion-associated proteins such as paxillin [33]. An examination of the localization of  $\beta$ 1-integrin by immunohistochemical staining revealed that  $\beta$ 1-integrin is highly localized to the periphery of the cell in the gels with fast stress relaxation, while  $\beta$ 1-integrin is diffusive throughout the cell in the gels with slow stress relaxation (Fig. 6A and B) [15]. Furthermore, integrin clusters in the fast-relaxing gels were found to be associated with paxillin localization, suggesting them to be focal adhesions (Fig. 6C). In addition, immunoblot analysis revealed that cells in gels with fast stress relaxation exhibited higher levels of phosphorylated focal adhesion kinase (FAK) and paxillin, indicative of higher levels of activation, relative to those in gels with slow stress relaxation (Supplementary Fig. 6). These findings indicate that the formation of integrin-based adhesions is improved in alginate-PEG gels.

Finally, we tested how stress relaxation in PEG-alginate gels regulates osteogenic differentiation of a murine mesenchymal stem cell line (D1, MSCs). A previous study established that faster relaxation promotes osteogenic differentiation of MSCs [11]. As osteogenic differentiation of MSCs requires an initial modulus of 11–30 kPa, the initial modulus of hydrogels was adjusted to ~15 kPa by increasing the concentration of calcium crosslinker (Fig. 7, A-C) [34]. MSCs were encapsulated in slow relaxing gels, which did not contain PEG, and in fast relaxing gels, with a high concentration of PEG. Markers of osteogenesis including alkaline phosphatase (ALP), osteocalcin (OCN), and bone sialoprotein (BSP) are up-regulated in the alginate-PEG gels, though runt-related transcription factor 2 (RUNX2), an early marker of osteogenesis, does not show any difference (Fig. 7D). Furthermore, the level of osteogenesis, as indicated by alkaline phosphatase staining, was found to increase in fast relaxing alginate-PEG gels, while decreasing in the gels without PEG (Fig. 7, E and F). These findings indicate that alginate-PEG gels can serve as a hydrogel platform to regulate stem cell differentiation.

## Discussion and Conclusions

In summary, we have demonstrated a simple but precise materials approach to tuning stress relaxation in alginate hydrogels, independently of an initial elastic modulus, via modulation of PEG molecular weight and density and calcium crosslinking. We show that grafting of commercially available PEG to commercially available alginate allows faster relaxation with increasing density or molecular weight of PEG. A previous study has found that that grafting of PEG onto alginate enhanced stress relaxation in hydrogels, but only considered one condition (DS2 of 5kDa PEG) and used low molecular weight alginate [11]. In this work, we rigorously explore how modulation of PEG density and molecular weight can be used to control stress relaxation using high molecular weight alginate. Interestingly, we found that total amount of PEG grafting onto alginate determines the rate of stress relaxation, and that there is no correlation between relaxation time and the length or the density of PEG when

total amount of PEG is held constant. Our interpretation is that while increased length of PEG chains would promote faster stress relaxation due to increased interactions with crosslinking zones in the alginate, the lower density of PEG chains, when the total amount of PEG is held constant, would diminish stress relaxation and compensate for that effect.

The utility of alginate-PEG gels as a 3D cell culture platform was also demonstrated. Previous studies developing viscoelastic hydrogels have established that hydrogels with fast stress relaxation promote cell spreading and osteogenesis [11,14,15]. Fast relaxing alginate-PEG gels in this work also allowed cell spreading and facilitated osteogenesis, as shown in the previous studies. While cells may not be able to fully spread in mesenchymal fashion in the fast-relaxing alginate-PEG hydrogels, they are able to spread to a greater extent in these gels than in the slow-relaxing hydrogels. Previous studies in 3D hydrogels have found osteogenic differentiation independent of cell spreading in hydrogels [37], and that cell spreading is not sufficient to drive osteogenic differentiation of MSCs [38]. One advantage of alginate-PEG gels is that the calcium concentrations needed for the gels to hold a similar initial modulus do not vary substantially, even at high concentrations of PEG (Supplementary Table 4). Therefore, these gels may be particularly useful to the application where low calcium variation is required. This method provides a simple and new approach to tuning viscoelasticity of hydrogels. This set of hydrogels may serve as a powerful materials platform to better mimic biophysical cues in ECM and thereby help elucidate the role of mechanical cues in cell biology in 3D cell culture.

## Supplementary Material

Refer to Web version on PubMed Central for supplementary material.

## Acknowledgments

We thank Prof. M. Levenston for the use of rheometer. This work was supported by a Samsung Scholarship for S.N., and a grant from the National Institutes of Health (1R21AR074070-01) to O.C.

## References

- [1]. Lutolf MP, Hubbell JA, Synthetic biomaterials as instructive extracellular microenvironments for morphogenesis in tissue engineering, *Nat. Biotechnol* 23 (2005) 47–55. doi:10.1038/nbt1055. [PubMed: 15637621]
- [2]. Langer R, Tirrell DA, Designing materials for biology and medicine, *Nature* 428 (2004) 487–492. [PubMed: 15057821]
- [3]. Healy KE, Reznick A, Stile RA, Designing Biomaterials to Direct Biological Responses, *Ann. N. Y. Acad. Sci* 875 (1999) 24–35. [PubMed: 10415555]
- [4]. Nguyen KT, West JL, Photopolymerizable hydrogels for tissue engineering applications, *Biomaterials* 23 (2002) 4307–4314. [PubMed: 12219820]
- [5]. Burdick JA, Anseth KS, Photoencapsulation of osteoblasts in injectable RGD-modified PEG hydrogels for bone tissue engineering, *Biomaterials* 23 (2002) 4315–4323. [PubMed: 12219821]
- [6]. Levental I, Georges PC, Janmey PA, Soft biological materials and their impact on cell function, *Soft Matter* 3 (2007) 299–306. doi:10.1039/B610522J.
- [7]. DuFort CC, Paszek MJ, Weaver VM, Balancing forces: architectural control of mechanotransduction., *Nat. Rev. Mol. Cell Biol* 12 (2011) 308–319. doi:10.1038/nrm3112. [PubMed: 21508987]

- [8]. Discher DE, Janmey P, Wang Y-L, Tissue cells feel and respond to the stiffness of their substrate., *Science* 310 (2005) 1139–1143. doi:10.1126/science.1116995. [PubMed: 16293750]
- [9]. Liu AP, Chaudhuri O, Parekh SH, New advances in probing cell–extracellular matrix interactions, *Integr. Biol* 9 (2017) 383–405. doi:10.1039/C6IB00251J.
- [10]. Yeh Y, Corbin EA, Caliarì SR, Ouyang L, Truitt R, Han L, Margulies KB, Burdick JA, Mechanically dynamic PDMS substrates to investigate changing cell environments, 145 (2017) 23–32. doi:10.1016/j.biomaterials.2017.08.033.
- [11]. Chaudhuri O, Gu L, Klumpers D, Darnell M, Bencherif SA, Weaver JC, Huebsch N, Lee H, Lippens E, Duda GN, Mooney DJ, Hydrogels with tunable stress relaxation regulate stem cell fate and activity, *Nat. Mater* 15 (2015) 326–334. doi:10.1038/nmat4489. [PubMed: 26618884]
- [12]. Nam S, Hu KH, Butte MJ, Chaudhuri O, Strain-enhanced stress relaxation impacts nonlinear elasticity in collagen gels, *Proc. Natl. Acad. Sci* 113 (2016) 5492–5497. doi:10.1073/pnas.1523906113. [PubMed: 27140623]
- [13]. Chaudhuri O, Gu L, Darnell M, Klumpers D, a Bencherif S, Weaver JC, Huebsch N, Mooney DJ, Substrate stress relaxation regulates cell spreading, *Nat. Commun* 6 (2015) 1–7. doi:10.1038/ncomms7365.
- [14]. McKinnon DD, Domaille DW, Cha JN, Anseth KS, Biophysically defined and cytocompatible covalently adaptable networks as viscoelastic 3d cell culture systems, *Adv. Mater* 26 (2014) 865–872. doi:10.1002/adma.201303680. [PubMed: 24127293]
- [15]. Lou J, Stowers R, Nam S, Xia Y, Chaudhuri O, Stress relaxing hyaluronic acid-collagen hydrogels promote cell spreading, fiber remodeling, and focal adhesion formation in 3D cell culture, *Biomaterials* 154 (2018) 213–222. doi:10.1016/j.biomaterials.2017.11.004. [PubMed: 29132046]
- [16]. Brown TE, Carberry BJ, Worrell BT, Dudaryeva OY, McBride MK, Bowman CN, Anseth KS, Photopolymerized dynamic hydrogels with tunable viscoelastic properties through thioester exchange, *Biomaterials* (2018) 1–8. doi:10.1016/j.biomaterials.2018.03.060.
- [17]. Nam S, Chaudhuri O, Mitotic cells generate protrusive extracellular forces to divide in three-dimensional microenvironments, *Nat. Phys* 14 (2018) 621–628. doi:10.1038/s41567-018-0092-1.
- [18]. Lee HP, Gu L, Mooney DJ, Levenston ME, Chaudhuri O, Mechanical confinement regulates cartilage matrix formation by chondrocytes, *Nat. Mater* 16 (2017) 1243–1251. doi:10.1038/nmat4993. [PubMed: 28967913]
- [19]. Cameron AR, Frith JE, Cooper-white JJ, The influence of substrate creep on mesenchymal stem cell behaviour and phenotype., *Biomaterials* 32 (2011) 5979–5993. doi:10.1016/j.biomaterials.2011.04.003. [PubMed: 21621838]
- [20]. Wisdom KM, Adebowale K, Chang J, Lee JY, Nam S, Desai R, Rossen NS, Rafat M, West RB, Hodgson L, Chaudhuri O, Matrix mechanical plasticity regulates cancer cell migration through confining microenvironments, *Nat. Commun* (2018). doi:10.1038/s41467-018-06641-z.
- [21]. Zhao X, Huebsch N, Mooney DJ, Suo Z, Stress-relaxation behavior in gels with ionic and covalent crosslinks, *J. Appl. Phys* 107 (2010) 1–5. doi:10.1063/1.3343265.
- [22]. Chaudhuri O, Viscoelastic hydrogels for 3D cell culture, *Biomater. Sci* 5 (2017) 1480–1490. doi:10.1039/c7bm00261k. [PubMed: 28584885]
- [23]. Dankers PYW, Harmsen MC, Brouwer Li.A., Van Luyn MJA, Meijer EW, A modular and supramolecular approach to bioactive scaffolds for tissue engineering, *Nat. Mater* 4 (2005). doi:10.1038/nmat1418.
- [24]. Highley CB, Rodell CB, Burdick JA, Direct 3D Printing of Shear-Thinning Hydrogels into Self-Healing Hydrogels, *Adv. Mater* 27 (2015) 5075–5079. doi:10.1002/adma.201501234. [PubMed: 26177925]
- [25]. Kloxin CJ, Scott TF, Adzima BJ, Bowman CN, Covalent Adaptable Networks ( CANs ): A Unique Paradigm in Cross-Linked Polymers, *Macromolecules* 43 (2010) 2643–2653. doi:10.1021/ma902596s. [PubMed: 20305795]
- [26]. Dooling LJ, Buck ME, Bin Zhang W, Tirrell DA, Programming Molecular Association and Viscoelastic Behavior in Protein Networks, *Adv. Mater* (2016) 4651–4657. doi:10.1002/adma.201506216. [PubMed: 27061171]

- [27]. Lou J, Liu F, Lindsay CD, Chaudhuri O, Heilshorn SC, Xia Y, Dynamic Hyaluronan Hydrogels with Temporally Modulated High Injectability and Stability Using a Biocompatible Catalyst, *Adv. Mater* (2018). doi:10.1002/adma.201705215.
- [28]. Malz F, Jancke H, Validation of quantitative NMR, *J. Pharm. Biomed. Anal* 38 (2005) 813–823. doi:10.1016/j.jpba.2005.01.043. [PubMed: 15893442]
- [29]. Reed S, Wu BM, Biological and mechanical characterization of chitosan-alginate scaffolds for growth factor delivery and chondrogenesis, *2* (2015) 272–282. doi:10.1002/jbm.b.33544.
- [30]. Zhang YS, Khademhosseini A, *Advances in engineering hydrogels*, *Science* 356 (2017). doi: 10.1126/science.aaf3627.
- [31]. Nam S, Lee J, Brownfield DG, Chaudhuri O, Viscoplasticity Enables Mechanical Remodeling of Matrix by Cells, *Biophys. J* 111 (2016) 2296–2308. doi:10.1016/j.bpj.2016.10.002. [PubMed: 27851951]
- [32]. Rowley JA, Madlambayan G, Mooney DJ, Alginate hydrogels as synthetic extracellular matrix materials, *Biomaterials* 20 (1999) 45–53. [PubMed: 9916770]
- [33]. Owen LM, Adhikari AS, Patel M, Grimmer P, Leijnse N, Kim MC, Notbohm J, Franck C, Dunn AR, A cytoskeletal clutch mediates cellular force transmission in a soft, three-dimensional extracellular matrix, *Mol. Biol. Cell* 28 (2017) 1959–1974. doi:10.1091/mbc.E17-02-0102. [PubMed: 28592635]
- [34]. Huebsch N, Arany PR, Mao AS, Shvartsman D, Ali OA, Bencherif SA, Rivera-feliciano J, Mooney DJ, Harnessing traction-mediated manipulation of the cell/matrix interface to control stem-cell fate, *Nat. Mater* 9 (2010) 518–526. doi:10.1038/nmat2732. [PubMed: 20418863]
- [35]. Ma Z, Lebard DN, Loverde SM, Sharp KA, Klein ML, Discher DE, Finkel TH, TCR Triggering by pMHC Ligands Tethered on Surfaces via Poly ( Ethylene Glycol ) Depends on Polymer Length, *PLoS One* 9 (2014) 1–10. doi:10.1371/journal.pone.0112292.
- [36]. Vold IMN, Kristiansen KA, Christensen BE, A Study of the Chain Stiffness and Extension of Alginates , in Vitro Epimerized Alginates , and Periodate-Oxidized Alginates Using Size-Exclusion Chromatography Combined with Light Scattering and Viscosity Detectors, *Biomacromolecules* 7 (2006) 2136–2146. doi:10.1021/bm060099n. [PubMed: 16827580]
- [37]. Huebsch N, Arany PR, Mao AS, Shvartsman D, Ali OA, Bencherif SA, Rivera-feliciano J, Mooney DJ, Harnessing traction-mediated manipulation of the cell/matrix interface to control stem-cell fate, *Nat. Mater* 9 (2010) 518–526. doi:10.1038/nmat2732. [PubMed: 20418863]
- [38]. Khetan S, Guvendiren M, Legant WR, Cohen DM, Chen CS, Burdick JA, Degradation-mediated cellular traction directs stem cell fate in covalently crosslinked three-dimensional hydrogels, *Nat. Mater* 12 (2013) 458–465. doi:10.1038/nmat3586. [PubMed: 23524375]

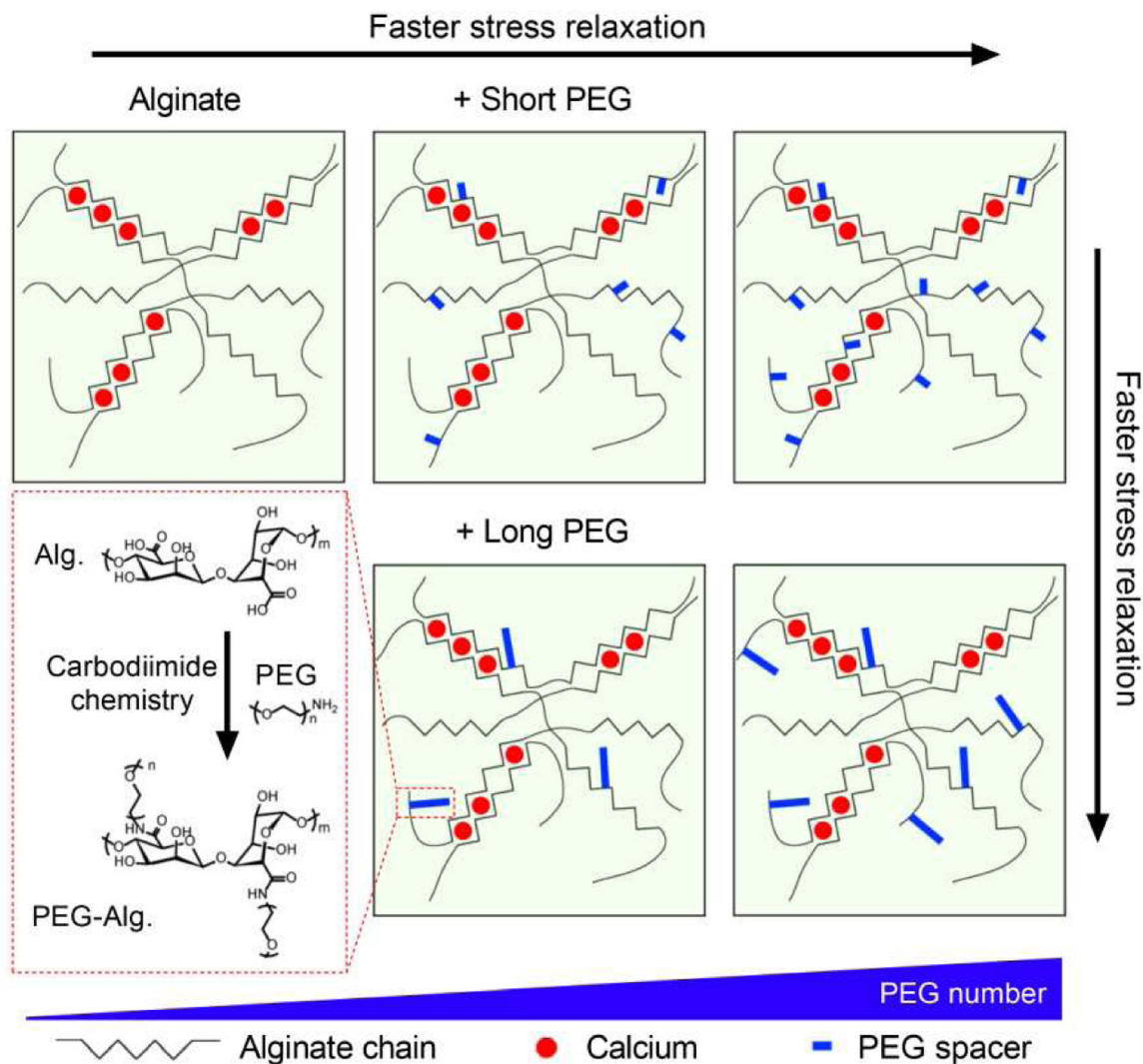


**Figure 1. Varying PEG molecular weight and number to tune stress relaxation in alginate-PEG hydrogels.**

A schematic depicting molecular structures of alginate-PEG hydrogel. Alginate polymers are grafted with various length and number of PEG through Carbodiimide chemistry. Alginate-PEG polymers are then crosslinked with Calcium. PEG acts as a spacer to provide a steric spacing of crosslinking zones in alginate. Increasing the number and length of PEG is predicted to increase stress relaxation rate.



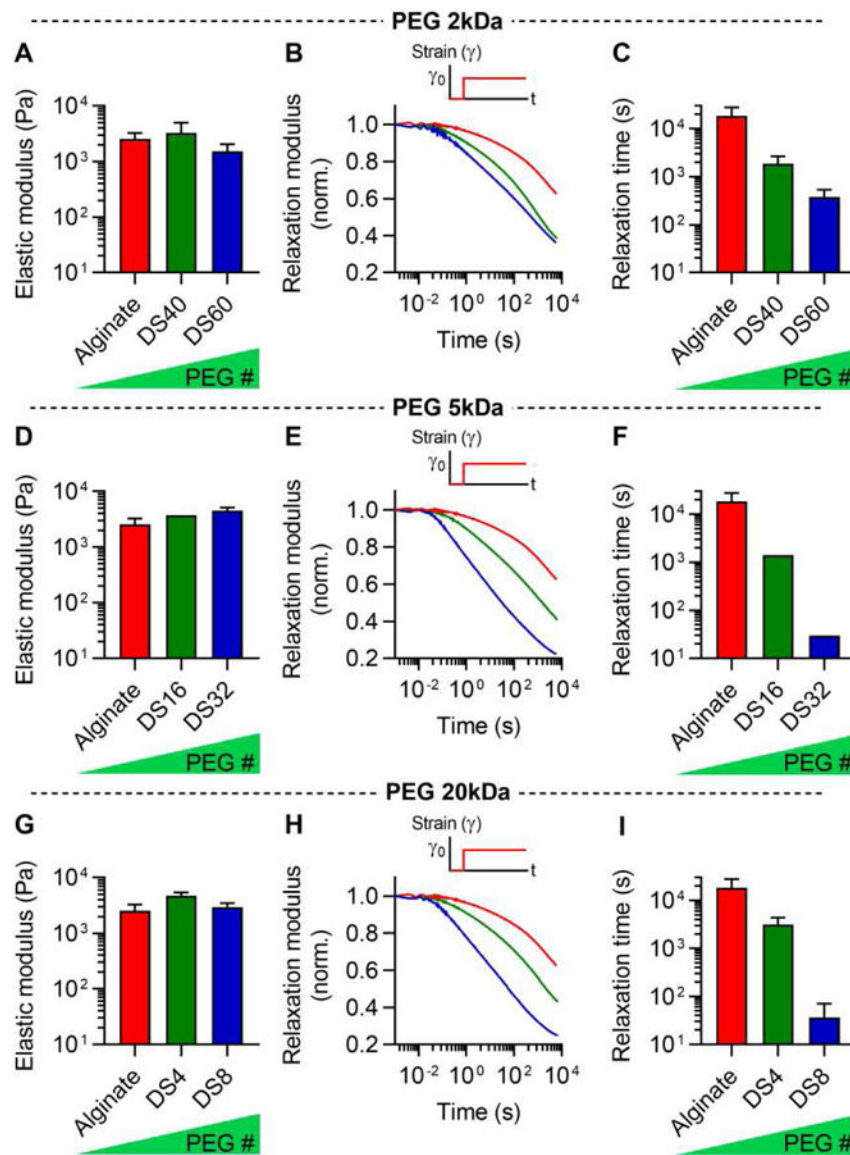


**Figure 2. Hydrogels of alginate grafted with increasing PEG concentration exhibit faster stress relaxation.**  
**A**, Initial elastic modulus of alginate grafted with 2kDa-PEG with degree of substitution (DS) 40 and 60. **B**, Stress relaxation tests for alginate-PEG hydrogels in **A**. **C**, Quantification of timescale at which the stress is relaxed to half its original value, relaxation time, from stress relaxation tests in **B**. **D**, Initial elastic modulus of alginate grafted with 5kDa-PEG with DS 16 and 32. **E**, Stress relaxation tests for alginate-PEG hydrogels in **D**. **F**, Quantification of relaxation time from stress relaxation tests in **E**. **G**, Initial elastic modulus of alginate grafted with 20kDa-PEG with DS4 and 8. **H**, Stress relaxation tests for alginate-PEG hydrogels in **G**. **I**, Quantification of relaxation time from stress relaxation tests in **G**.



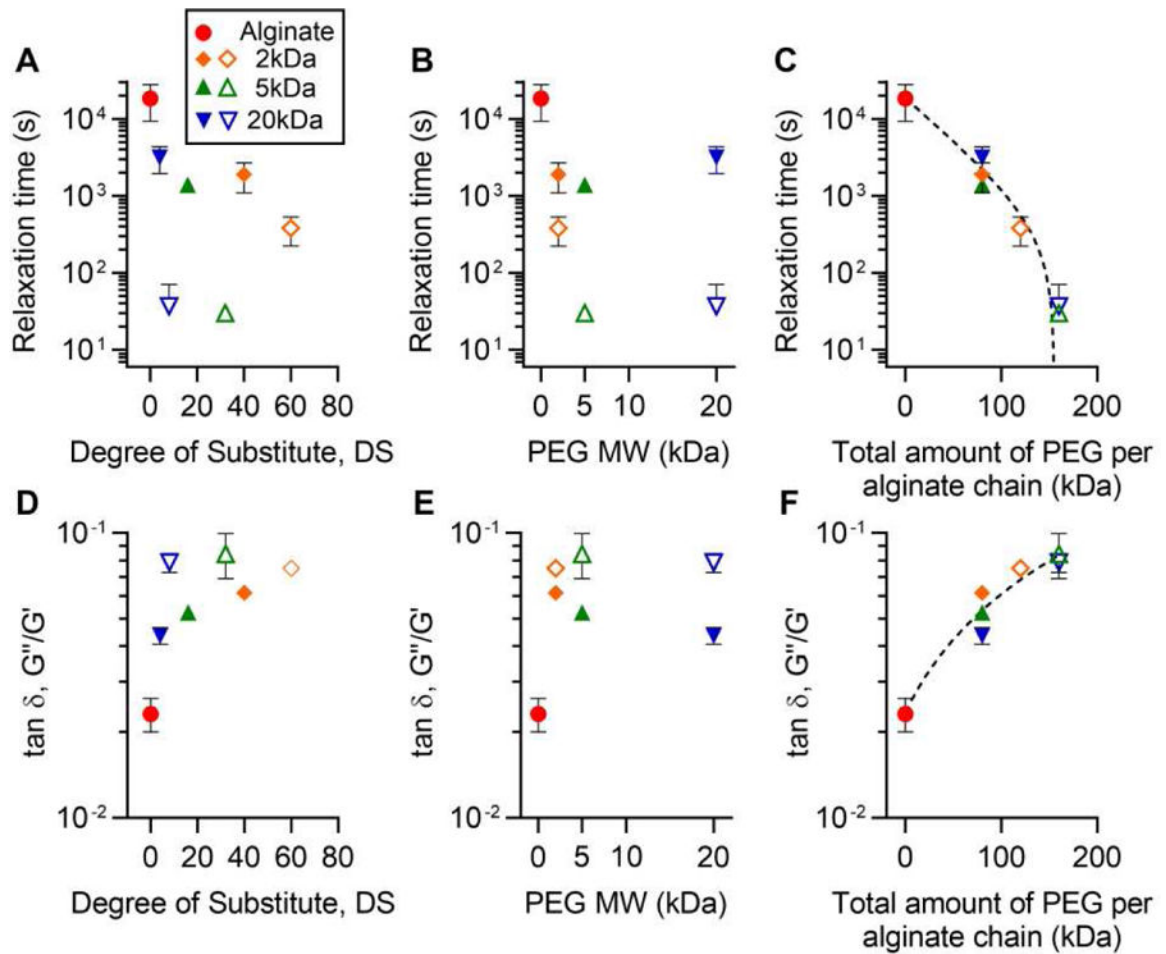


**Figure 3. Total mass amount of PEG in alginate-PEG gels determines hydrogel stress relaxation and loss tangent.**

Display of relaxation time as a function of **A**, degree of substitution (DS), **B**, length, and **C**, the total amount of PEG. In C, relaxation time was fitted as  $y = 18904 e^{-0.025x} - 402$ .

Display of loss tangent, a measure of viscosity defined as the ratio of loss modulus ( $G''$ ) to storage modulus ( $G'$ ), as a function of **A**, DS, **B**, length, and **C**, the total amount of PEG. In F, loss tangent was fitted as  $y = 3.75 \times 10^{-4x} + 0.0236$ .

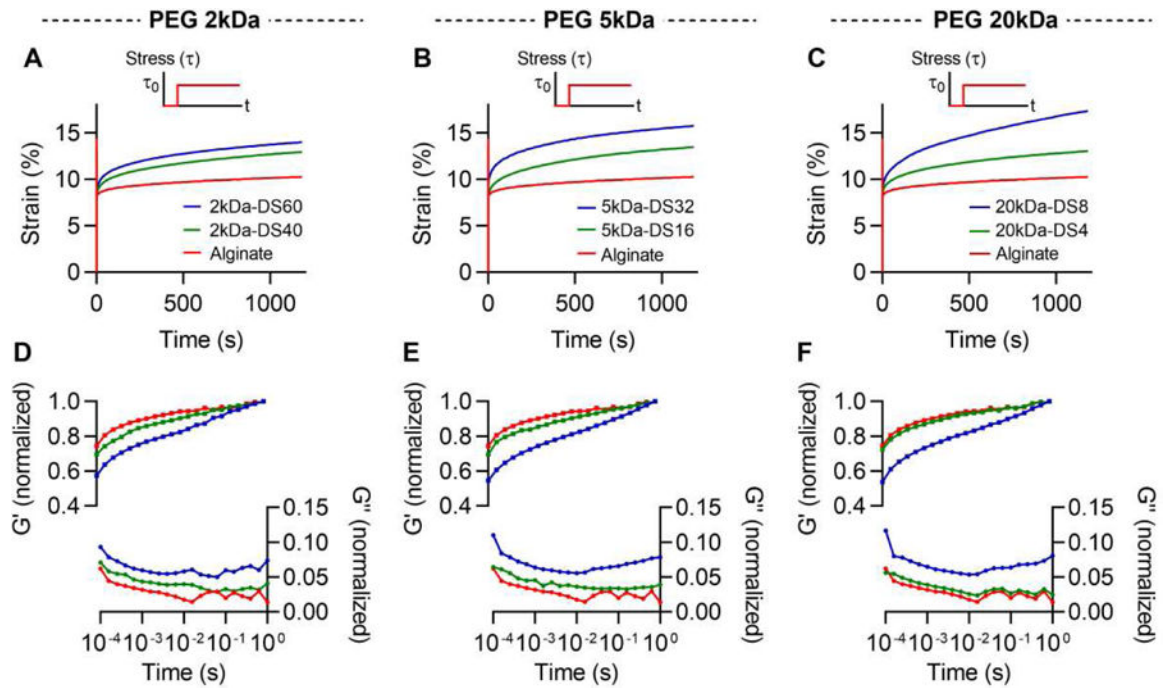


**Figure 4. Increasing PEG mass in alginate-PEG gels enhances creep and leads to a higher loss modulus.**

Creep tests for gels of alginate grafted with **A**, 2, **B**, 5, and **C**, 20 kDa of PEG. Frequency-dependent tests for gels of alginate with **A**, 2, **B**, 5, and **C**, 20 kDa of PEG. Storage modulus and loss modulus were normalized by the storage modulus at 1 Hz.

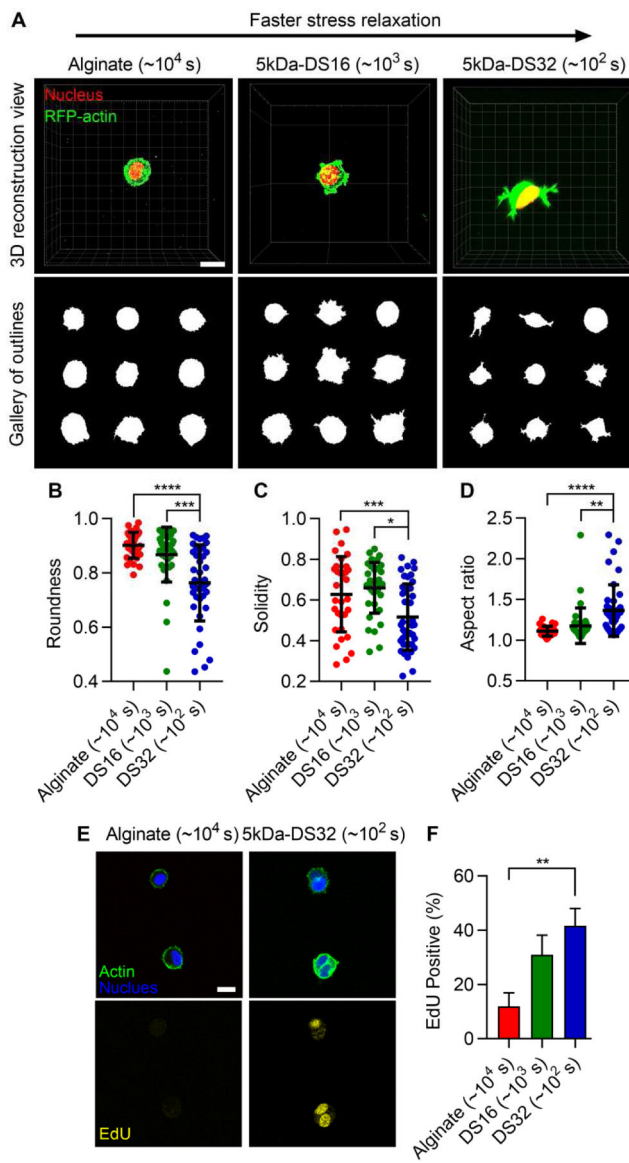


**Figure 5. Faster stress relaxation in alginate-PEG hydrogels promotes cell spreading and cell-cycle progression.**  
**A**, Morphologies of 3T3 fibroblasts encapsulated within alginate gels without, and with 5k Da PEG of DS 16 and 32. Red and green represent nucleus and actin. Quantification of **B**, roundness, **C**, solidity, and **D**, aspect ratio of cells in the alginate-PEG gels. **E**, Fluorescent images of cells for EdU staining. **F**, Quantification of EdU positive cells in alginate-PEG gels. One-way ANOVA and Tukey’s comparisons; \*, \*\*, \*\*\*, and \*\*\*\* indicate  $p < 0.05$ ,  $p < 0.01$ ,  $p < 0.001$ , and  $p < 0.0001$ , respectively. Scale bars are 10  $\mu\text{m}$ .

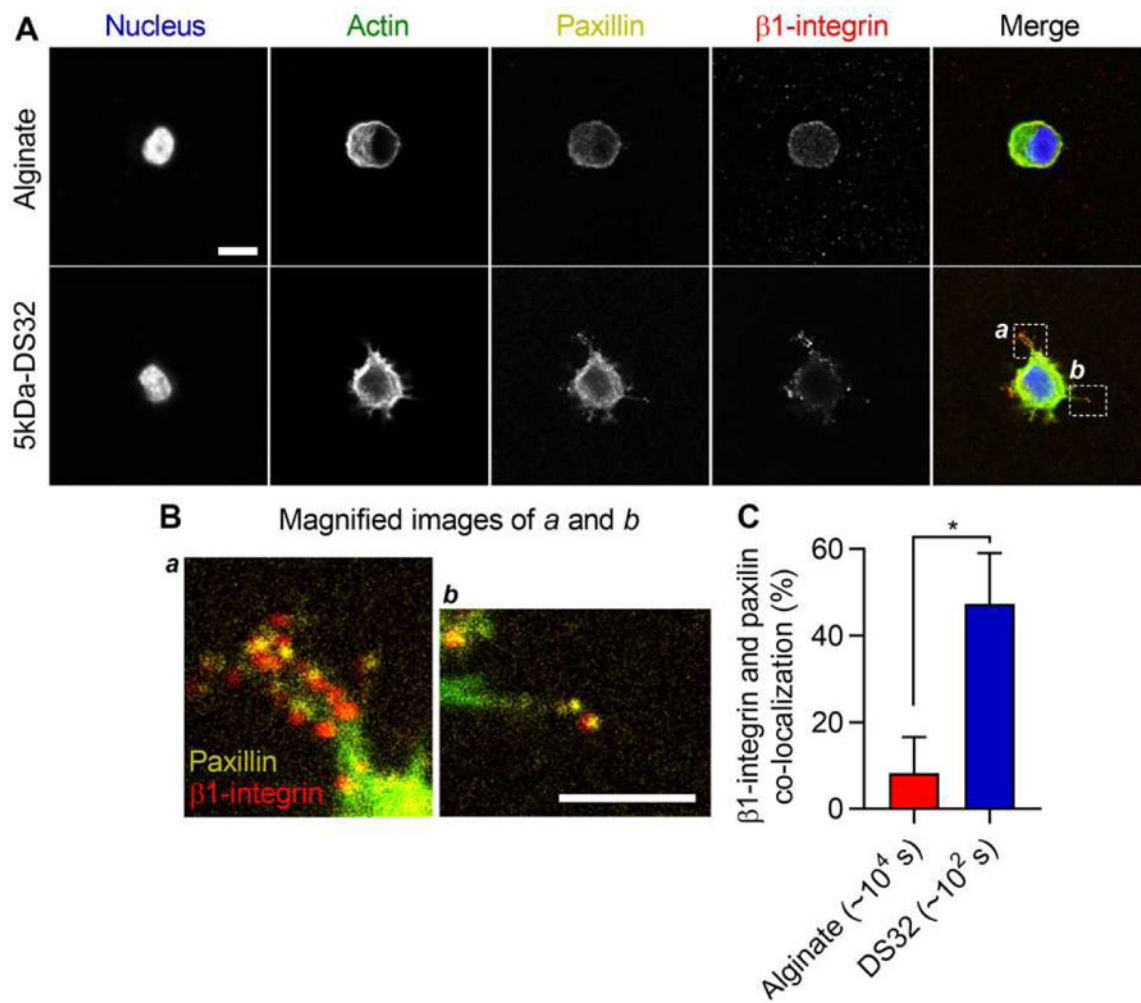


**Figure 6. Paxillin and  $\beta 1$ -integrin are co-localized at the periphery of cells in gels with faster stress relaxation.**

**A**, Fluorescent images of paxillin and  $\beta 1$ -integrin in cells within alginate-PEG gels. **B**, Magnified images of region of interests specified in **A**. Yellow and red represent paxillin and  $\beta 1$ -integrin. Scale bars are 10  $\mu\text{m}$ . **C**, Quantification of co-localization of paxillin and  $\beta 1$ -integrin. Student t-tests; \* indicates  $p < 0.05$ .

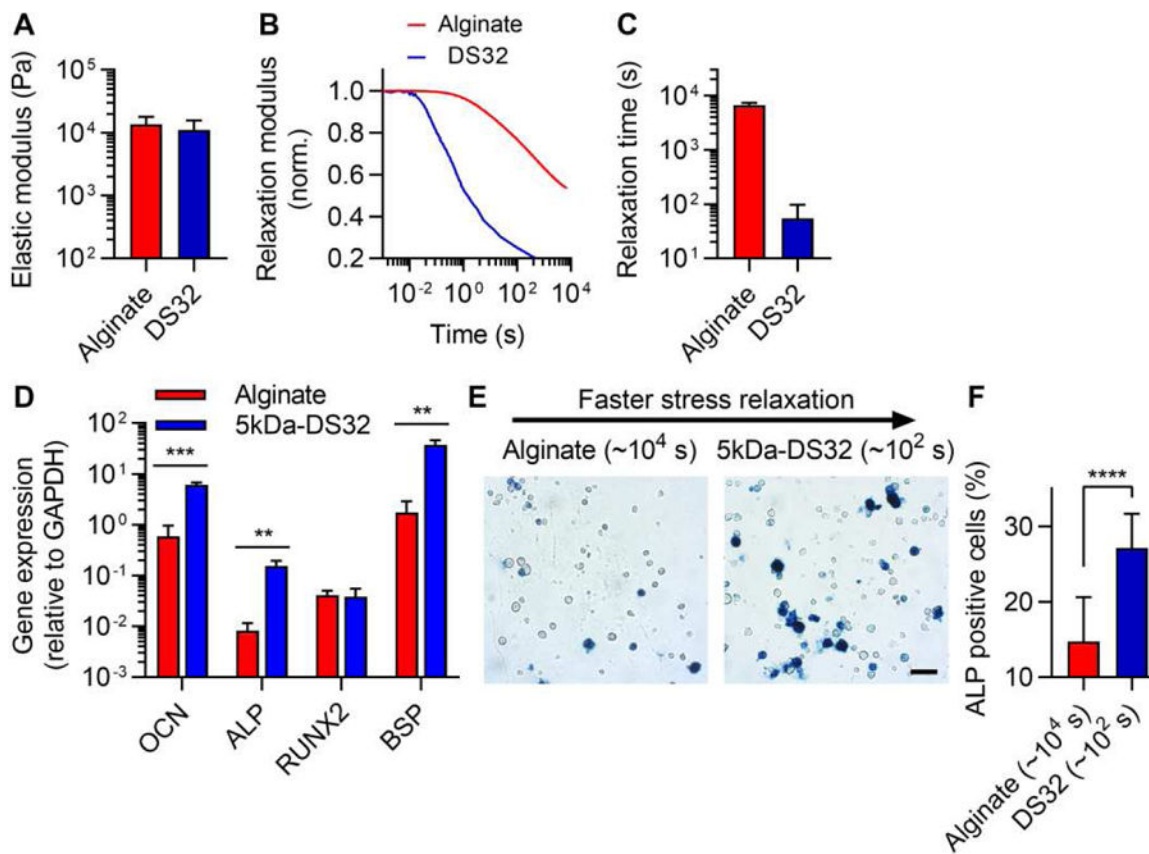


**Figure 7. Mesenchymal stem cells (MSCs) undergo enhanced osteogenic differentiation in alginate-PEG gels relative to alginate gels.**

**A**, Initial elastic modulus of stiff alginate-PEG gels for osteogenesis study. **B**, Stress relaxation tests for stiff alginate-PEG hydrogels. **C**, Quantification of relaxation time from stress relaxation tests. **D**, The expression of markers of osteogenesis including *OCN*, *ALP*, *RUNX2* and *BSP*. **E**, Images of alkaline phosphatase staining (ALP, blue), indicating early osteogenic differentiation, for MSCs cultured in alginate-PEG gels for seven days. **F**, Quantification of ALP positive cells. Student t-tests; \*\*, \*\*\*, and \*\*\*\* indicate  $p < 0.01$ ,  $p < 0.001$ , and  $p < 0.0001$ , respectively. Scale bar is 50  $\mu\text{m}$ .